

Dynamical mechanism of antifreeze proteins to prevent ice growth

B. Kutschen¹, K. Morawetz^{1,2,3}, S. Thoms⁴

¹ *Münster University of Applied Science, Stegerwaldstrasse 39, 48565 Steinfurt, Germany*

² *International Institute of Physics (IIP) Federal University of Rio Grande do Norte Av. Odilon Gomes de Lima 1722, 59078-400 Natal, Brazil*

³ *Max-Planck-Institute for the Physics of Complex Systems, 01187 Dresden, Germany and*

⁴ *Alfred Wegener Institut, Am Handelshafen 12, D-27570 Bremerhaven, Germany*

The fascinating ability of algae, insects and fishes to survive at temperatures below normal freezing is realized by antifreeze proteins (AFPs). Antifreeze proteins (AFPs) are surface-active molecules and interact with the diffusive water/ice interface preventing a complete solidification. A new dynamical mechanism is proposed how these proteins inhibit the freezing of water. We apply a Ginzburg-Landau type approach to describe the phase separation in the two-component system (ice, AFP). The free energy density involves two fields: one for the ice phase with low AFP concentration, and one for the liquid water with high AFP concentration. The time evolution of the ice reveals microstructures as a result of phase separation in the presence of AFPs. We observe a faster clustering of pre-ice structure connected with a locking of grain size by the action of AFP which is an essentially dynamical process. The adsorption of additional water molecules are inhibited and the further growth of ice grains are stopped. The interfacial energy between ice and water is lowered by which the AFPs allow only smaller critical ice nucleus to be formed. Similar to a hysteresis in magnetic materials we observe a thermodynamic hysteresis leading to a nonlinear density dependence of the freezing point depression in agreement with the experiments.

PACS numbers: 87.15.kr, 05.70.Fh, 64.60.Ej, 87.15.A-

I. INTRODUCTION

The suppression of freezing temperature by antifreeze proteins (AFPs) which allows fishes and diatoms to survive even below 0 °C is a fascinating phenomenon. There are four classes (I-IV) of antifreeze proteins with wide structural diversity and size, a class of antifreeze glycoproteins (AFGPs) and a number of hyperactive antifreeze proteins in insects [1, 2] as illustrated in figure 1. The great diversity of molecular structures is visible and consequently the influence of the structural diversity on the antifreeze activity and grain growth [3] has to be considered. Experimental results illustrate a connection between protein structure and the thermal hysteresis activity on the one hand [4, 5], and between the protein structure and the ice growth patterns on the other [3, 6].

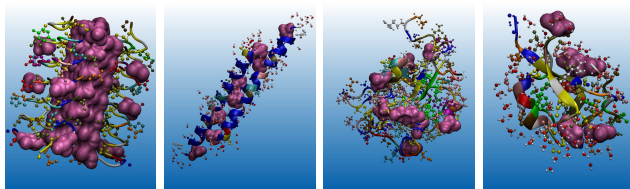


FIG. 1: Four different classes of AFP structures (from left to right): tenebrio molitor (1EZG), psodeupleuronectes americanus (1WFB), hemitripterus americanus (2AFP), and macrozoarces americanus (1MSI). Crystallographic data are from the RCSB Protein Data Bank.

The mechanism of AFP binding is still unresolved [7] since the details of the antifreeze effect are difficult to test experimentally in vivo, mainly because it is not easy to access them in their natural environment. Molecular

dynamics simulations [5, 8] are limited by the computing power and running times. Moreover the interaction between AFPs and the liquid-solid interface is considerably determined by the choice of the water model and the potential parameters [9–17]. The simple freezing point depression like in saline solutions is proportional to the molal concentration of the solute molecule [18] which colligative property does not depend on the structure of the molecule. However a more careful inspection of AFPs shows a nonlinear dependence such that colligative mechanisms are ruled out [5]. We want to propose a dynamical mechanism for freezing point depression by AFPs leading to a nonlinear dependence on the AFP density.

There is not a single mechanism known up to date which explains the AFP ice-binding affinity and specificity [1]. One reason lies in the considerable variation of the primary, secondary and tertiary structure of AFPs [1, 2, 7, 18–20] because the ice-binding affinity depends on the molecular recognition according to the key-lock principle [21, 22]. The different kinds of structures lead to various kinetic models of AFP activity [4, 23–28]. A significant difference can be found by the shape of the antifreeze activity between AFGP 4 and AFGP 8 [4, 29]. In addition to that, several authors have substituted threonine residues and investigated the influence on the thermal hysteresis [30, 31] or have enhanced the activity of a β -helical antifreeze protein by engineered addition of coils [32, 33]. Moreover, other authors have assessed the relationship between the noncolligative freezing point depression and the molecular weight of AFPs [31, 34] and have observed cooperative functioning between the larger and the smaller components [35]. The stabilization of supercooled fluids by thermal hysteresis proteins [36, 37] is

discussed with a number of models based on kinetics, statistical mechanics and homogeneous or inhomogeneous nucleation [23, 24, 26–29, 33, 34, 38–41].

All the described models provide a thermal hysteresis as a function of concentration, but no pattern formation in space and time during the phase transition from liquid water to ice. In contrast, the Turing model [42] and the phase field model [43] simulate the morphology of the microstructure growth but without thermal hysteresis. Our main goal is to include kinetic models capable to describe the experimental observations into the phase field method and to justify the non-equilibrium stabilized supercooled liquid state of the hysteresis. The main question is what mechanism stabilizes the difference between the melting and freezing point and establishes the hysteresis. We use coupled phase field equations for the water-ice structure and the AFP concentration which is sophisticatedly connected with the question how the protein structure will influence the antifreeze activity. We will calculate the dynamical formation of the micro-structures by solving the coupled phase field equations which combine the phase field theory of Caginalp [44–49], Cahn and Hilliard [50–53] with various kinetics [4, 18, 26, 27, 33]. In the next section we outline shortly the basic equations and models. Then we present the nonlinear freezing point depression from static conditions and support it by numerical discussions of the time-dependence of freezng suppression.

II. COUPLING OF AFP TO ICE STRUCTURE

Due to the lack of complete understanding of water by first principles it is also possible to start with a phase field model [50] with ice nucleation of Cahn-Hilliard-type proposed in [51]. We identify the ice structure by an order parameter u describing the "tetrahedrality" [54]

$$u \sim 1 - M_T = 1 - \frac{1}{15 \langle l^2 \rangle} \sum_{i,j} (l_i - l_j)^2, \quad (1)$$

where l_i are the lengths of the six edges of the tetrahedron formed by the four nearest neighbors of the considered water molecule. For an ideal tetrahedron one has $M_T = 0$ and the random structure yields $M_T = 1$. In this way it is possible to discriminate between ice- and water molecules either by a two-state continuous function. Other authors prefer the "tetrahedrality" in order to define the order parameter [55–57]. We adopted a quartic order parameter relationship of Ginzburg-Landau-type for the free energy density

$$f(u, v) \sim \beta u + \lambda u^2 - 2\lambda u^3 + \lambda u^4 + c \left(\frac{\partial u}{\partial x} \right)^2 \quad (2)$$

allowing nonlinear structures to be formed. The fourth order function enables a double well potential for the description of the water-ice phase transition [58]. The

coefficient λ describes the free energy density scale and β the deviation from equilibrium.

The versatile action of different molecular structures of AFPs on the grain growths will be simulated by an activity parameter relating the structural order parameter with the antifreeze concentration $f(u, v) \sim -a_1 uv$. The coefficient a_1 describes the interaction between the order parameter u and the antifreeze concentration v . This approach is different from the description of simple freezing point depression in saline solutions [43] in that the AFPs act analogously to a magnetic field on charged particles providing a hysteresis.

We follow the philosophy of the conserving Cahn-Hilliard equation and assume that the time-change of the order parameter is proportional to the gradient of a current $\dot{u} = -\nabla j$. The current itself is assumed to be a generalised force which in turn is given by the gradient of a potential, $j \sim \nabla \Phi$. The latter one is the variation of the free energy such that finally $\dot{u} = -\nabla^2 \left(-\frac{\partial f}{\partial u} \right)$ results. From the differential form for a general continuity equation $\frac{\partial v}{\partial t} + \frac{\partial j}{\partial x} = 0$ with the AFP field v and the flux $j = -\frac{\partial}{\partial x} (a_3 v + a_2 u)$ we get a diffusion equation $\frac{\partial v}{\partial t} = \frac{\partial^2}{\partial x^2} (a_2 u + a_3 v)$ as evolution for the AFP concentration. For further considerations we introduce dimensionless quantities $\tau = \frac{t}{t_0}$, $\xi = \frac{x}{x_0}$, $u = C_1 \hat{\psi}$, $v = C_2 \rho$, with $C_1 = 1$, $C_2 = \frac{a_1}{12\lambda}$, $x_0 = \frac{1}{6} \sqrt{\frac{6c}{\lambda}}$, $t_0 = \frac{c}{72\lambda^2}$ with $\alpha_1 = \frac{a_1^2}{12^2 \lambda^2}$, $\alpha_2 = \frac{a_2}{12\lambda}$ and $\alpha_3 = \frac{c\beta}{72\lambda^2}$ such that the order-parameter and AFP concentration equations read

$$\frac{\partial \psi}{\partial \tau} = \frac{\partial^2}{\partial \xi^2} \left(\alpha_3 + \left(\frac{1}{6} - a + a^2 \right) \psi + \left(a - \frac{1}{2} \right) \psi^2 + \frac{1}{3} \psi^3 - \alpha_1 \rho - \frac{\partial^2 \psi}{\partial \xi^2} \right) \quad (3)$$

$$\frac{\partial \rho}{\partial \tau} = \frac{\partial^2}{\partial \xi^2} (\psi + \alpha_2 \rho). \quad (4)$$

We have shifted $\psi = \hat{\psi} - a$ by technical reasons since $a = 1/2$ allows to remove the cubic term in the free energy.

The Cahn-Hilliard equation cannot be derived from the Onsager reciprocal theorem [59] because the Markovian condition is not satisfied [60], but has the virtue of a conserving quantity. It possesses a stationary solution which can be seen from the time evolution of the total free energy [61]

$$\begin{aligned} \frac{d}{dt} \int f dV &= \int \frac{\delta f}{\delta \psi} \frac{d\psi}{dt} dV = \int \frac{\delta f}{\delta \psi} \nabla^2 \left(\frac{\partial f}{\partial \psi} \right) dV \\ &= - \int \left(\nabla \frac{\partial f}{\partial \psi} \right)^2 dV \leq 0. \end{aligned} \quad (5)$$

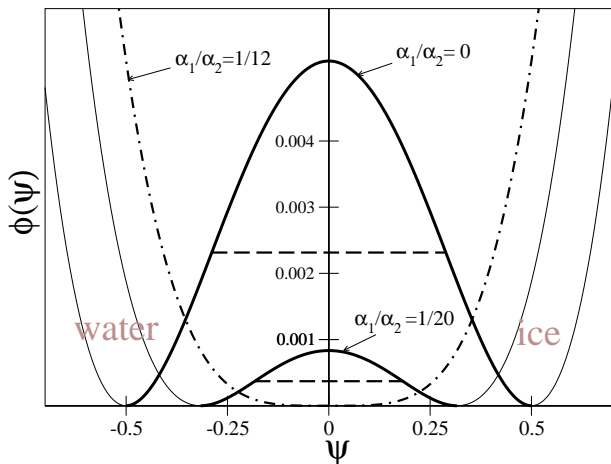


FIG. 2: Free energy density (solid) versus order parameter for different AFP concentrations, pure ice/water $\frac{\alpha_1}{\alpha_2} = 0$ (upper line). The freezing transition interval is given by $\partial^2\phi/\partial\psi^2 = 0$ (dashed lines).

III. MECHANISM OF FREEZING POINT DEPRESSION

A. Phase diagram

We analyze the static solution of (3) and (4) eliminating $\rho = -\psi/\alpha_2$ and obtain

$$\frac{\partial^2\psi}{\partial\xi^2} = \alpha_3 - \aleph\psi - \left(a - \frac{1}{2}\right)\psi^2 + \frac{1}{3}\psi^3 \equiv \frac{\partial\phi}{\partial\psi} \quad (6)$$

which can be understood as the Euler-Lagrange equations from the free energy

$$\begin{aligned} f &= \alpha_3\psi - \aleph\frac{\psi^2}{2} + \left(a - \frac{1}{2}\right)\frac{\psi^3}{3} + \frac{1}{12}\psi^4 + \frac{1}{2}\left(\frac{\partial\psi}{\partial\xi}\right)^2 \\ &\equiv \phi + \frac{1}{2}\left(\frac{\partial\psi}{\partial\xi}\right)^2 \end{aligned} \quad (7)$$

and we abbreviate $\aleph = -\frac{1}{6} + a - a^2 - \frac{\alpha_1}{\alpha_2}$. Eq. 6 is easily integrate by multiplying both sides with $\partial\psi/\partial\xi$ to yield

$$\frac{1}{2}\left(\frac{\partial\psi}{\partial\xi}\right)^2 = \phi + c \equiv \Phi \quad (8)$$

providing the virial theorem $f = 2\phi + c = 2\Phi - c = (\psi')^2 - c$ as an expression for the conservation of energy. This fact allows one to calculate the static profile of the kink solution as we will see. Depending on the parameter of α_1/α_2 and α_3 we can have an asymmetric potential Φ describing the thermodynamic hysteresis though α_3 does not influence the dynamics due to the differentiation in Eq. (3). Near the phase transition the potential Φ becomes symmetric and possesses a reflection symmetry $\Phi(\psi) = \Phi(-\psi)$ with the minima $\psi_{min} = \pm\sqrt{3\aleph}$. Hence,

the constant c can be found from the condition $\Phi(\sqrt{3\aleph}) = -\frac{3}{4}\aleph^2 + c = 0$.

In figure 2 the symmetric potential is plotted where the left and right minima reflect the stable phase of water and ice respectively. The concave $\partial^2\Phi/\partial\psi^2 < 0$ region corresponds to a negative diffusion coefficient leading to structure formation. The flux diffuses up against the concentration gradient contrary to the Onsager reciprocal theorem [59] and which is the unstable phase transition region. This freezing region is shrunk by the AFP concentration where for $\frac{\alpha_1}{\alpha_2} = \frac{1}{12}$ the double well vanishes.

B. Linear stability analysis

It is also possible to compute the phase transition region with the help of the positive eigenvalues μ of the linear stability analysis around the equilibrium value $\psi = \psi_0 + \psi_0 \exp(\mu\tau + i\kappa\xi)$ and $\rho = \rho_0 + \rho_0 \exp(\mu\tau + i\kappa\xi)$ with the wavenumber κ and the fixed point ψ_0 . Each fixed point describes a spatial homogeneous order parameter $\psi = \psi_0 = const$ and corresponds to a stationary solution of water or ice. For pure water ($\alpha_1 = 0$) of (3) the range of unstable homogeneous solution is

$$\mu^*(\kappa) = (\aleph - \psi_0^2)\kappa^2 - \kappa^4 > 0 \quad (9)$$

and a perturbation grows in time and therefore establishes a spatial structure. For the complete equation system (3) and (4) with thermal hysteresis proteins (AFPs), we obtain the eigenvalues

$$\mu(\kappa) = -\frac{1}{2}(\alpha_2\kappa^2 - \mu^*(\kappa)) \pm \frac{1}{2}\sqrt{(\alpha_2\kappa^2 + \mu^*(\kappa))^2 - 4\alpha_1\kappa^4}. \quad (10)$$

The region of positive eigenvalues corresponds to the freezing (spinodal) region. The unstable modes vanish for $\psi_0^2 > 1/12$ and so the double well too for $\alpha_1/\alpha_2 > 1/12$. A phase transition occurs only, if the fixed points are located inside of $-1/\sqrt{12} < \psi_0 < 1/\sqrt{12}$ being also inside the freezing (spinodal) interval in Fig. 2. Since $\sqrt{\aleph} = \psi_0$ at the inflection points it can be concluded from Eq. (9)

$$\kappa^2 + \psi_0^2 - \left(\frac{1}{12} - \frac{\alpha_1}{\alpha_2}\right)\psi_0 < 0 \quad (11)$$

forming an elliptic paraboloid as phase diagram in figure 3. The size of the microstructure is coupled to the AFP concentration and to the order parameter ψ_0 which decides how much ice and water is present. The freezing region shrinks with increasing AFP concentration and vanishes at $\alpha_1/\alpha_2 = 1/12$.

C. Surface energy depression

The virtue of the Cahn Hilliard equation (3) is the existence of a transient stationary solution by integrating

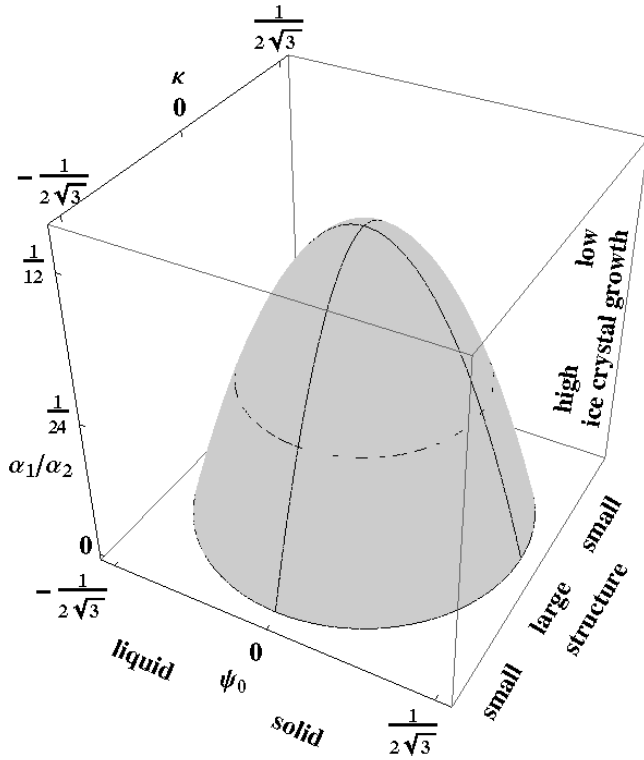


FIG. 3: Freezing (spinodal) region dependent on the order parameter ψ_0 and the wavenumbers κ and the thermal hysteresis activity $\frac{\alpha_1}{\alpha_2}$.

(8) in form of a kink solution

$$\psi(\xi) = -\sqrt{3\aleph} \tanh \left[\sqrt{\aleph/2}(\xi - \xi_0) \right] \quad (12)$$

with $\aleph = \frac{1}{12} - \frac{\alpha_1}{\alpha_2}$ as plotted in figure 4. The corresponding interfacial energy density of the kink is easily evaluated using the centered free energy density $\epsilon(\xi) = f(\xi) - c = \left(\frac{\partial\psi}{\partial\xi}\right)^2$ plotted as well in figure 4.

One recognizes that the presence of AFPs reduces the kink between water and ice and lowers the interfacial energy density. This is already a static mechanism which shows how the AFPs inhibit the ice formation on large time scales. The interfacial surface energy (tension)

$$\zeta = \int_{-\infty}^{\infty} \epsilon(\xi) d\xi = (2\aleph)^{3/2} \quad (13)$$

is decreasing with increasing AFP coupling to vanish at the critical value $\alpha_1/\alpha_2 = 1/12$ which is the limit of the stability region. Transforming back to the dimensional interfacial energy one obtains $6^{3/2}\gamma\zeta$ with our choice of the surface tension $\gamma = 21.9 \frac{mJ}{m^2}$ [51]. Direct and indirect measurements provide values which vary between $20 \frac{mJ}{m^2}$ and $46 \frac{mJ}{m^2}$ [62]. In contrast to antifreeze proteins γ increases linearly with salt concentration and a larger critical nucleus is required in order to generate an interface compared to pure water. Salt inhibits the nucleation process because of the higher energy threshold

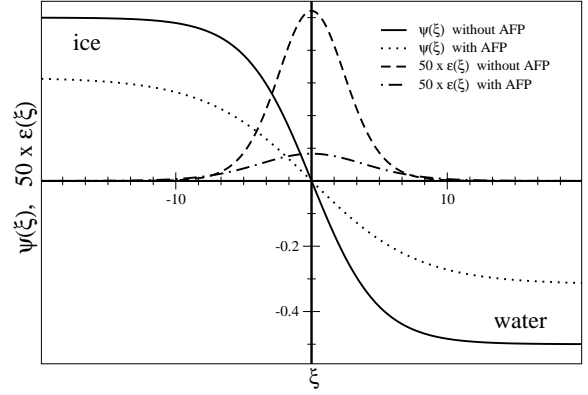


FIG. 4: Static kink solution (12) and the interfacial energy density $\epsilon(\xi)$ on the interface with AFPs ($\frac{\alpha_1}{\alpha_2} = 0.05$) and without AFPs ($\frac{\alpha_1}{\alpha_2} = 0$).

whereas thermal hysteresis proteins (AFP) reduce the threshold for a stable nucleus. From this effective surface tension one might fix the ratio of materials parameter $\aleph = 1/12 - \alpha_1/\alpha_2$.

An ice crystal forms when the aqueous phase undergoes supercooling below the freezing point. In the supercooled phase water can transform from the aqueous to the solid phase by the growth of nucleation kernels if a critical size is exceeded. Within a simple liquid drop model the volume part of Gibb's potential is negative $\sim -4\pi r^3 \Delta G_V / 3$ while the surface part contributes positively $\sim 4\pi r^2 \zeta$. Therefore Gibb's potential exhibits a maximum at the critical cluster size $r^* = 2\zeta / \Delta G_V$. As long as $r < r^*$ nucleation might happen (embryo) but no cluster grows for which case the critical cluster size has to be exceeded. This interfacial energy of the critical nucleus and the degree of supercooling are essentially influenced by the AFPs. Indeed the change of the free energy between ice and water $\psi(\pm\infty) = \pm\sqrt{3\aleph}$ reads with the stationary solution (12)

$$\Delta F = -2(\alpha_3 - \alpha_1\rho)\sqrt{3\aleph} \approx \Delta G_V. \quad (14)$$

With (13) the critical (dimensionless) radius $r^* = \sqrt{2\aleph}/3(\alpha_1\rho - \alpha_3)$ decreases as the AFP concentration α_1/α_2 increases. In other words many AFPs allow many ice nucleations but inhibit the cluster growth.

D. Freezing point depression

The decrease of the freezing temperature ΔT can be estimated by the change of the free energy during the phase transition since the corresponding minima of the asymmetric free energy are nearly the same as the ones of the symmetric free energy (14). We can write

$$\Delta F|_{\text{ice-water}} = \left. \frac{\partial F}{\partial T} \right|_{\text{ice}} \Delta T \quad (15)$$

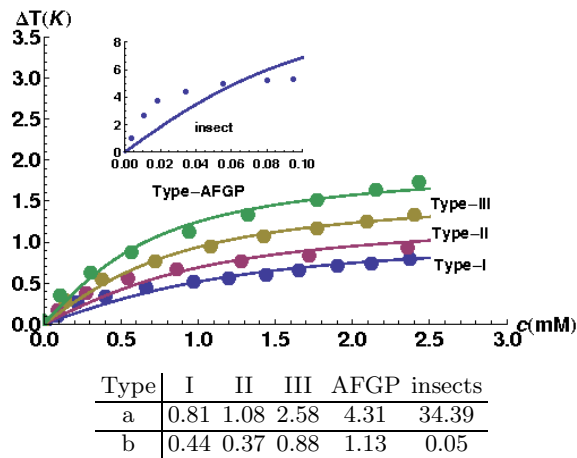


FIG. 5: The freezing temperature depression of four different classes of AFP structures and insects versus AFP concentration where (16) is used (lines) to fit the experimental data (points) of [5]. The AFP-specific fitting parameter are given in the table.

for constant particles number and pressure. We model the temperature dependence of the coupling between AFP concentration and ice structure as $\alpha_1(T) = \alpha_0 + \alpha_{10}(T - T_c^0)$ with some internal threshold temperature T_c^0 . The activity of AFP molecules will certainly be temperature dependent and cease to act at the critical temperature $\alpha_1(T^*) = 0$. Therefore the freezing point depression is given by $\Delta T = T^* - T_c^0$. Introducing the AFP-dependent supercooling temperature $T_c = T_c^0 - |\Delta T|$ one may write $\alpha_1(T) = \alpha_0(T - T_c)/|\Delta T|$. From (15) and (14) we obtain the freezing point depression or thermodynamical hysteresis observing that $\psi|_{\text{ice}} = \sqrt{3N}$

$$|\Delta T| = \sqrt{\left(\frac{b}{2\rho}\right)^2 + a} - \frac{b}{2\rho} \quad (16)$$

with $a = 2\alpha_0(T - T_c)/\alpha_{10}$ and $b = 2\alpha_3/\alpha_{10}$. We see a nonlinear square root behaviour of the freezing point depression in dependence on the AFP concentration ρ which expands for small concentrations $|\Delta T| \approx \frac{a}{b}\rho = \frac{\alpha_0}{\alpha_3}(T - T_c)\rho$ into a colligative freezing depression analogously as known from saline solutions. The nonlinear behaviour fits well with the experiments as seen in figure 5. The fit parameters can be translated into two conditions for the four materials parameter $\alpha_3, \alpha_{10}, \alpha_0$ and T_c for each specific AFP. Together with the surface tension our approach leaves one free parameter to describe further experimental constraints.

E. Time evolution of ice growth inhibition

Now that we have seen how the AFP reduces the interfacial energy and therefore the formation of ice crystals we want to investigate the time evolution. We use the exponential time differencing scheme of second or-

der (ETD2) [63] with the help of which a stiff differential equation of the type $y' = ry + z(y, t)$ with a linear term ry and a nonlinear part $z(y, t)$ can be integrated. The linear equation is solved formally and the integral over the nonlinear part is approximated by a proper finite differencing scheme. The time evolution of the coupled equations (3) are seen in figure 6. Due to the conserving Cahn Hilliard equation we have conservation of total mass density of water ρ_w but a relative redistribution between water ρ_{liq} and ice ρ_{ice} densities which read in terms of the ice order parameter $\rho_w(\xi, t) = \rho_{liq}[1 - \psi(\xi, t)] + \rho_{ice}[1 + \psi(\xi, t)]$. Since the total integral over the order parameter $\int \psi(\xi, t)d\xi = const$ the mass conservation of water is ensured.

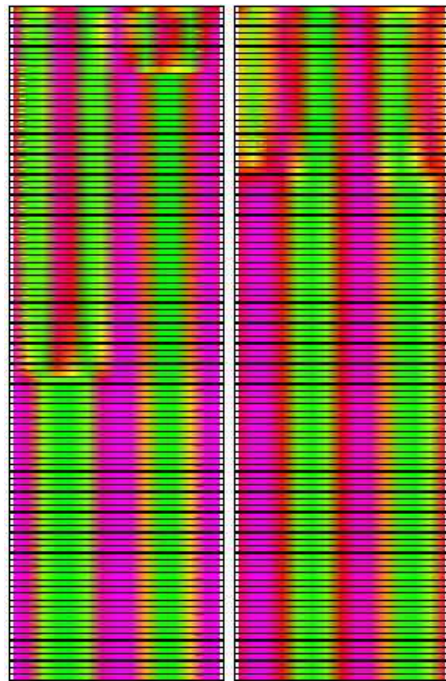


FIG. 6: Time evolution of the order parameter versus length from 1×10^5 to 2×10^6 time steps (from above to below), left side without AFPs and right side with AFPs.

In figure 6 we plot the time evolution of an initially small-scale distributed sinusoidal order parameter with and without AFPs. The evolution equations obviously reduce the number of ice grains forming a larger one after some time. Interestingly this accretion occurs faster with AFPs than without. However, as we have seen already the absolute height of the ice-order parameter (ideal ice corresponds to $\Psi = 1$) is lowered during this process by AFPs.

This is also illustrated by the time-evolution of the half width of the kinks in figure 7 which we interpret as the size of the ice grains. One sees that the grain size of ice evolves faster with AFPs and remains at a smaller value compared to the case without AFPs. This means the nucleation of ice starts earlier with AFPs but remains locked at an intermediate stage. This is in agreement with the

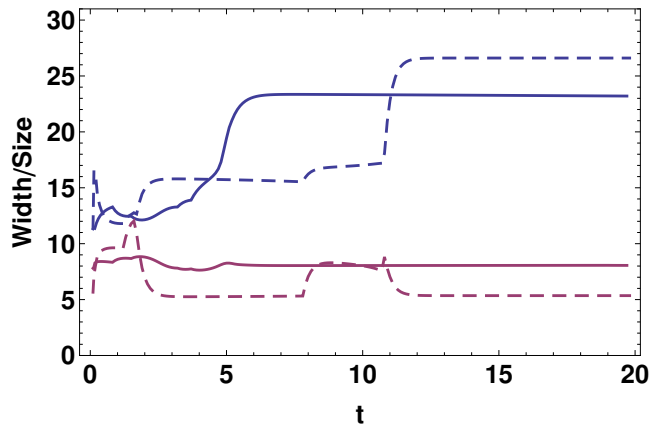


FIG. 7: The half width of ice structure (upper curves) together with the thickness of the boundary (lower curves) without (dashed) and with AFPs (solid) of the time evolution of order parameter from figure 6.

static observation above that the AFPs support smaller nuclei sizes and inhibit the cluster growth. Accompanied with this observation we see also that the width of the boundary between ice and water remains larger with AFPs than without. This is of course an expression of

the reduction of interfacial energy.

IV. SUMMARY

The interaction of AFP molecules with ice crystals are described by a coupled phase field equation between the order parameter describing ice and water and the AFP concentration. We find essentially two effects of AFPs to suppress the formation of ice. First the interfacial energy is lowered which allows only smaller ice nucleus to be formed. And secondly we see that the ice grains are faster formed by the action of AFPs but become locked at smaller sizes and smaller order parameters. The latter means that the freezing is stopped and ice-water mixture remains instead of complete freezing. This essentially dynamical process between AFP structure and ice-order parameter establishes a new possible mechanism for the phenomenon of anti-freeze proteins. We demonstrate that the model is capable to reproduce the experimental data on the freezing point depression.

This work was supported by DFG-priority program SFB 1158. The financial support by the Brazilian Ministry of Science and Technology is acknowledged.

-
- [1] J. Barrett, *IJBCB* **33**, 105 (2001).
 [2] Z. Jia and P. L. Davies, *TRENDS in Biochemical Sciences* **27**, 101 (2002).
 [3] Y. Yeh, R. E. Feeney, R. L. McKown, and C. J. Warren, *Measurement of Grain Growth* **34**, 1495 (1994).
 [4] T. S. Burcham, D. T. Osuga, Y. Yeh, and R. E. Feeney, *J. Biol. Chem.* **261**, 6390 (1986).
 [5] H. Nada and Y. Furukawa, *Polymer Journal* **44**, 690 (2012).
 [6] M. Bar-Dolev, Y. Celik, J. S. Wettlaufer, P. L. Davies, and I. Braslavsky, *J. R. Soc. Interface* **9**, 3249 (2012).
 [7] C. L. Hew and D. S. C. Yang, *Eur. J. Biochem* **203**, 33 (1992).
 [8] J. J. Liu, Y. Qin, M. B. Dolev, Y. Celik, J. S. Wettlaufer, and I. Braslavsky, *Proc. R. Soc. A* **468**, 3311 (2012).
 [9] B. Guillot, *Journal of Molecular Liquids* **101**, 219 (2002).
 [10] H. J. C. Berendsen, J. R. Grigera, and T. P. Straatsma, *J. Phys. Chem.* **91**, 6269 (1987).
 [11] H. J. C. Berendsen, J. P. M. Postma, W. F. van Gunsteren, A. DiNola, and J. R. Haak, *J. Chem. Phys.* **81**, 3684 (1984).
 [12] I. M. Svishchev and P. G. Kusalik, *J. Am. Chem. Soc.* **118**, 649 (1996).
 [13] W. L. Jorgensen, J. Chandrasekhar, J. D. Madura, R. W. Impey, and M. L. Klein, *J. Chem. Phys.* **79**, 926 (1983).
 [14] P. T. Kiss and A. Baranyai, *J. Chem. Phys.* **134**, 054106 (2011).
 [15] H. A. Stern, F. Rittner, B. J. Berne, and R. A. Friesner, *J. Chem. Phys.* **115**, 2237 (2001).
 [16] M. W. Mahoney and W. L. Jorgensen, *J. Chem. Phys.* **112**, 8910 (2000).
 [17] U. Essmann, L. Perera, and M. L. Berkowitz, *J. Chem. Phys.* **103**, 8577 (1995).
 [18] Y. Yeh and R. E. Feeney, *Chem. Rev.* **96**, 601 (1996).
 [19] I. Grunwald, K. Rischka, S. M. Kast, T. Scheibel, and H. Bargel, *Phil. Trans. R. Soc. A* **367**, 1727 (2009).
 [20] M. M. Harding, L. G. Ward, and A. D. J. Haymet, *Eur. J. Biochem.* **264**, 653 (1999).
 [21] M. E. Daley, L. Spyrapoulos, Z. Jia, P. L. Davies, and B. D. Sykes, *Biochemistry* **41**, 5515 (2002).
 [22] E. K. Leinala, P. L. Davies, D. Doucet, M. G. Tyshenko, V. K. Walker, and Z. Jia, *J. Biol. Chem.* **227**, 33349 (2002).
 [23] Q. Z. Li, Y. Yeh, J. J. Liu, R. E. Feeney, and V. V. Krishnan, *J. Chem. Phys.* **124**, 204702 (2006).
 [24] L.-F. Li, X. Liang, and Q. Li, *Chem. Phys. Lett.* **472**, 124 (2009).
 [25] E. Kristiansen and K. E. Zachariassen, *Cryobiology* **51**, 262 (2005).
 [26] N. Kubota, *Cryobiology* **63**, 198 (2011).
 [27] S. Wang, N. Amornwittawat, and X. Wen, *J. Chem. Thermodynamics* **53**, 125 (2012).
 [28] L. M. Sander and A. V. Tkachenko, *Phys. Rev. Lett.* **93**, 128102 (2004).
 [29] Q. Li and L. Luo, *Chem. Phys. Lett.* **320**, 335 (2000).
 [30] W. Zhang and R. A. Laursen, *J. Biol. Chem.* **273**, 34806 (1998).
 [31] J. D. Schrag, S. M. O'Grady, and A. L. DeVries, *Biochimica et Biophysica Acta* **717**, 322 (1982).
 [32] C. B. Marshall, M. E. Daley, B. D. Sykes, and P. L. Davies, *Biochemistry* **43**, 11637 (2004).
 [33] Y. Mao and Y. Ba, *J. Chem. Phys.* **125**, 091102 (2006).
 [34] J. A. Raymond and A. L. de Vries, *PNAS* **74**, 2589 (1977).

- [35] D. T. Osuga, F. C. Ward, Y. Yeh, and R. E. Feeney, *J. Biol. Chem.* **253**, 6669 (1978).
- [36] P. W. Wilson and J. P. Leader, *Biophysical Journal* **68**, 2098 (1995).
- [37] K. E. Zachariassen, *Physiological Reviews* **65**, 799 (1985).
- [38] Q. Li and L. Luo, *Chem. Phys. Lett.* **216**, 453 (1993).
- [39] Q. Li and L. Luo, *Chem. Phys. Lett.* **223**, 181 (1994).
- [40] J. Liu and Q. Li, *Chem. Phys. Lett.* **378**, 238 (2003).
- [41] J. Liu and Q. Li, *Chem. Phys. Lett.* **422**, 67 (2006).
- [42] B. Kutschan, K. Morawetz, and S. Gemming, *Phys. Rev. E* **81**, 036106 (2010).
- [43] S. Thoms, B. Kutschan, and K. Morawetz, *Journal of Glaciology* (2013), submitted.
- [44] G. Caginalp, *Arch. Rat. Mech. Anal.* **92**, 205 (1986).
- [45] G. Caginalp and J. T. Lin, *J. Appl. Math.* **39**, 51 (1987).
- [46] G. Caginalp and P. C. Fife, *J. Appl. Math.* **48**, 506 (1988).
- [47] G. Caginalp, *Phys. Rev. A* **39**, 5887 (1989).
- [48] G. Caginalp, *J. Appl. Math.* **44**, 77 (1990).
- [49] G. Caginalp, *Rocky Mountain Journal of Mathematics* **21**, 603 (1991).
- [50] L. Gránásy, T. Pusztai, and J. A. Warren, *J. Phys. Cond. Mat.* **16**, 1205 (2004).
- [51] L. Gránásy, *Journal of Molecular Structure* **485**, 523 (1999).
- [52] L. Gránásy and D. W. Oxtoby, *J. Chem. Phys.* **112**, 2410 (2000).
- [53] L. Gránásy, T. Pusztai, and P. F. James, *J. Chem. Phys.* **117**, 6157 (2002).
- [54] N. N. Medvedev and Y. I. Naberukhin, *J. Non-Cryst. Solids* **94**, 402 (1987).
- [55] J. R. Errington and P. G. Debenedetti, *Nature* **409**, 318 (2001).
- [56] P. Kumar and S. V. B. an H. Eugene Stanley, *PNAS* **106**, 22130 (2009).
- [57] P. E. Mason and J. W. Brady, *J. Phys. Chem. B* **111**, 5669 (2007).
- [58] P. R. Harrowell and D. W. Oxtoby, *J. Chem. Phys.* **86**, 2932 (1987).
- [59] A. A. Wheeler, in *Handbook of Crystal Growth*, edited by D. T. J. Hurle (North Holland, Amsterdam, London, New York, Tokyo, 1993), vol. 1b.
- [60] H. Emmerich, *The diffuse interface approach in materials science* (Springer-Verlag, Berlin, Heidelberg, 2003).
- [61] M. Bestehorn, *Hydrodynamik und Strukturbildung* (Springer-Verlag, Berlin, Heidelberg, 2006).
- [62] D. R. H. Jones, *Journal of Materials Science* **9**, 1 (1974).
- [63] S. M. Cox and P. C. Matthews, *J. Comp. Phys.* **176**, 430 (2002).